Breakdown voltage analysis of $Al_{0.25}Ga_{0.75}N$/GaN high electron mobility transistors with partial silicon doping in the AlGaN layer*

Duan Bao-Xing(段宝兴)[a)b)†] and Yang Yin-Tang(杨银堂)[a)b)]

[a)] *School of Microelectronics, Xidian University, Xi'an* 710071, *China*

[b)] *Key Laboratory of Wide Band Gap Semiconductor Materials and Devices of Ministry of Education, Xi'an* 710071, *China*

(Received 13 September 2011; revised manuscript received 9 January 2012)

In this paper, two-dimensional electron gas (2DEG) regions in AlGaN/GaN high electron mobility transistors (HEMTs) are realized by doping partial silicon into the AlGaN layer for the first time. A new electric field peak is introduced along the interface between the AlGaN and GaN buffer by the electric field modulation effect due to partial silicon positive charge. The high electric field near the gate for the complete silicon doping structure is effectively decreased, which makes the surface electric field uniform. The high electric field peak near the drain results from the potential difference between the surface and the depletion regions. Simulated breakdown curves that are the same as the test results are obtained for the first time by introducing an acceptor-like trap into the N-type GaN buffer. The proposed structure with partial silicon doping is better than the structure with complete silicon doping and conventional structures with the electric field plate near the drain. The breakdown voltage is improved from 296 V for the conventional structure to 400 V for the proposed one resulting from the uniform surface electric field.

Keywords: AlGaN/GaN, high electron mobility transistors (HEMTs), two-dimensional electron gas (2DEG), electric field modulation

PACS: 72.80.Ey, 72.80.Ga, 73.40.Lq **DOI:** 10.1088/1674-1056/21/5/057201

1. Introduction

Since the development of silicon power devices is limited in the high frequency, high temperature, and high power fields, wide band-gap semiconductor devices have become a hot research topic. The band gap of wide band-gap semiconductors is larger than 2.0 eV, and includes diamond, four-compound SiC, II–VI compound GaN and ternary compounds. These materials generally have a wide band-gap, high critical breakdown field, high thermal conductivity, high electron saturation velocity, and low intrinsic leakage current, are are suitable for devices with high-temperature, high-frequency, and high power, compared with devices based on silicon and narrow-band GaAs.[1,2] AlGaN/GaN high electron mobility transistors (HEMTs) are the core of the microwave signal amplification system due to their high-density two-dimensional electron gas (2DEG: 10^{13} cm^{-2}) and high electron mobility (about 2000 $cm^2/V{\cdot}s$), which can produce much higher RF power. For AlGaN/GaN HEMTs, the main areas of research include designing new structures with high breakdown voltage,[3−6] relieving self-heat and current collapse[7−9] via structural design and and reliability improvements.[10,11] To achieve a certain power density and specific power conversion in the power devices, the breakdown voltage is an important parameter. Researchers have proposed many methods and techniques to improve the breakdown voltage and decrease the specific on resistance.[12−18]

In this paper, new AlGaN/GaN HEMTs are proposed with partial silicon doping in the AlGaN layer. The silicon doping has modulated the concentration of the high density 2DEG, and a new electric field peak has been introduced in the AlGaN layer, which modulates the electric field distribution at the interface between the AlGaN and GaN buffer. The high electric field near the gate edge is reduced and the breakdown voltage is increased. The percentage of Al is 25% for the AlGaN layer.

*Project supported by the Young Scientists Fund of the National Natural Science Foundation of China (Grant No. 61106076).

†Corresponding author. E-mail: bxduan@163.com

© 2012 Chinese Physical Society and IOP Publishing Ltd

2. Device structure and description

AlGaN/GaN is a heterojunction including the AlGaN materials, with the larger band gap grown on the GaN buffer. The AlGaN is formed by epitaxy, and the polarization field is obtained from the positive charge of the AlGaN surface to the negative charge at the interface of the AlGaN and GaN buffer. In order to shield the polarization electric field, the high density 2DEG is formed at the conductive channel with the low barrier. This polarization includes the piezoelectric and spontaneous polarization. The total polarization charge can be expressed by

$$\begin{aligned}\sigma(x) = {} & P_{\text{spontaneous}}(\text{Al}_x\text{Ga}_{(1-x)}\text{N}) \\ & - P_{\text{spontaneous}}(\text{GaN}) \\ & + P_{\text{piezoelectric}}(\text{Al}_x\text{Ga}_{(1-x)}\text{N}) \\ & - P_{\text{piezoelectric}}(\text{GaN}). \end{aligned} \quad (1)$$

The break mechanism of the AlGaN/GaN HEMTs is different from the silicon devices with the PN junction or MOS system. The traditional silicon structure bears the voltage by the depletion region of the PN junction. This depletion region includes the negative charge and positively charged areas. The AlGaN/GaN HEMTs have formed a high polarization electric field in the AlGaN layer. The high density charge includes the AlGaN surface positive charge and 2DEG due to the polarization effects. The depletion layer is formed to bear the breakdown voltage from the charged state into the neutral state of the GaN buffer layer, which is adverse to traditional silicon power devices.

Figure 1 shows a new $Al_{0.25}Ga_{0.75}N$/GaN HEMTs structure with the part silicon doping in the middle of the AlGaN layer for the first time. A low barrier is introduced into the GaN surface to the bound electron. The electron can be injected into the low barrier when the partial silicon atoms are ionized and a positive charge is formed in the AlGaN layer. This is a mature technology for GaAs and AlGaN/GaN heterojunctions.[19−21] The different 2DEG regions from the gate to the drain electrodes are introduced by partial silicon doping in the AlGaN layer. The surface electric field of the AlGaN/GaN is modulated by the positive charge after the doped silicon is ionized. The high electric field near the gate of the AlGaN/GaN HEMTs is decreased due to the new electric field peak produced by the partial silicon doping, which improves the breakdown voltage. This is the kind of electric field modulation technique proposed in Refs. [14]–[18].

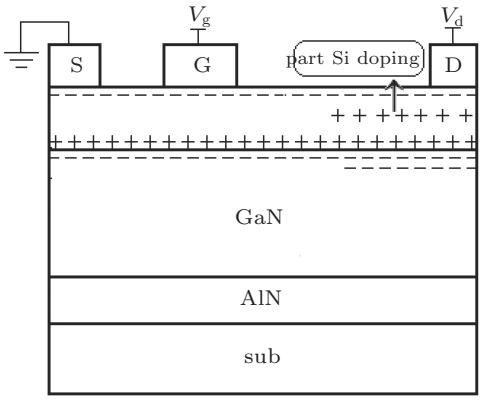


Fig. 1. Cross section of the partial silicon doping $Al_{0.25}Ga_{0.75}N$/GaN HEMTs.

3. Simulation results and discussion

The results were obtained by ISE simulation.[22] The parameters for the $Al_{0.25}Ga_{0.75}N$/GaN HEMTs with N-type impurities and acceptor-like traps into the GaN buffer are as follows. The thicknesses of the GaN buffer and AlGaN are 2.0 μm and 20 nm, respectively; the length from the source to the gate electrode (L_{gs}) is 1.0 μm; the length from the gate to the drain electrode (L_{gd}) is 8.0 μm; and the length of the gate electrode (L_g) is 1.0 μm.

The 2DEG of the $Al_{0.25}Ga_{0.75}N$/GaN HEMTs with partial silicon doping is formed by AlGaN layer doping and polarization effects. Two concentration regions are introduced from the gate to the drain electrodes. Figure 2 shows the 2DEG concentration of the proposed partial silicon doping $Al_{0.25}Ga_{0.75}N$/GaN HEMTs. Figure 2(a) is the lateral distribution of the 2DEG concentration. Because of the polarization effect for the $Al_{0.25}Ga_{0.75}N$/GaN heterostructure, a carrier with the concentration 7.3×10^{19} cm^{-3} is formed at the interface between the AlGaN and GaN. The carrier concentration near the drain is 8.4×10^{19} cm^{-3} due to partial silicon doping, which makes the drift region concentration gradient from the gate to drain electrodes. This kind of concentration gradient is similar to the drift region zoning for a silicon LDMOS (lateral double diffusion metal oxide semiconductor).[23,24] The silicon is defined to dope into the AlGaN layer using ISE simulation software.

Figure 2(b) shows the 2DEG vertical distribution at the low barrier channel region. It can be seen

that the 2DEG concentration of 8.4×10^{19} cm^{-3} is the highest at the interface between the AlGaN and GaN buffer. This concentration decreases gradually along the vertical direction, and the range is about 5 nm. By simple integral calculation, the 2DEG concentration is 2.1×10^{13} cm^{-2} and 1.8×10^{13} cm^{-2} for the partial silicon doping and conventional $Al_{0.25}Ga_{0.75}N$/GaN HEMTs, respectively.

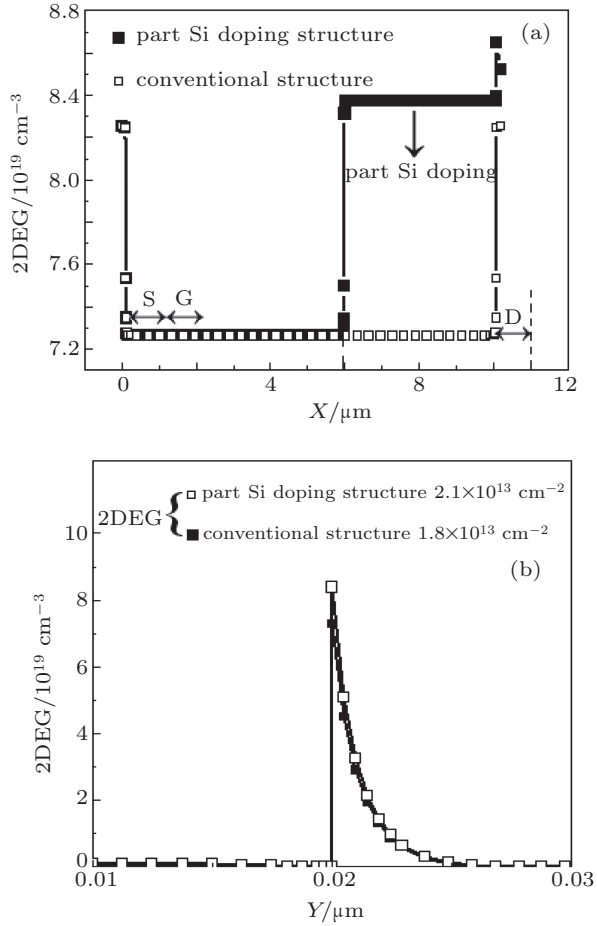


Fig. 2. The 2DEG of the $Al_{0.25}Ga_{0.75}N$/GaN HEMTs: (a) lateral distribution and (b) vertical distribution.

For the un-doped GaN buffer, the conductivity is N-type and the concentration is not less than 1.0×10^{15} cm^{-3}. An unintentionally doped GaN buffer, grown by both MOCVD and MBE, exhibits some degree of N-type conductivity due to the unintentional oxygen or silicon doping which results in buffer leakage current in the GaN-based electric devices.[25–29] When the drain electrode of the $Al_{0.25}Ga_{0.75}N$/GaN HEMTs is of positive bias, the output of I_{ds}–V_{ds} is an ohmic behavior due to the ohmic contact for the source and drain electrodes, even though the 2DEG is depleted, which can be seen from Fig. 3. Figure 3 shows the I_{ds}–V_{ds} for the $Al_{0.25}Ga_{0.75}N$/GaN HEMTs based on the doped GaN buffer with different N-type concentration. It can be seen that the I_{ds} is increased linearly with V_{ds}, which is an Ohmic characteristic.

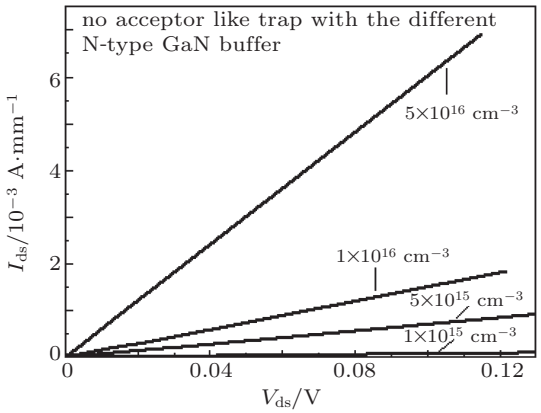


Fig. 3. I_{ds}–V_{ds} for the $Al_{0.25}Ga_{0.75}N$/GaN HEMTs without the acceptor-like trap.

In order to decrease the buffer leakage to improve the breakdown voltage, some deep levels have been introduced by the GaN MBE. The deep levels are the acceptor-like traps and can capture the electron emitted from the source electrode.[25–29] To obtain a breakdown behavior that is consistent with the examination curve, the acceptor-like trap is introduced into the GaN buffer. For the positive voltage of the drain electrode, the Schottky junction, formed by the gate and drain electrodes, is reverse biased. The electrons emitted from the source electrode to form the leakage current are captured by the acceptor-like trap. A breakdown curve that is the same as the test results is shown in Fig. 4, and is thanks to the acceptor-like trap. So, for the simulation of $Al_{0.25}Ga_{0.75}N$/GaN HEMTs, the acceptor-like trap is an important parameter. It can be seen from Fig. 4 that the I_{ds}–V_{ds} is a linear relationship for the $Al_{0.25}Ga_{0.75}N$/GaN HEMTs without the acceptor-like trap in the GaN buffer, which results from the source and drain ohmic contacts. When the acceptor-like trap is introduced into the GaN buffer, the leakage current due to the N-type GaN buffer is decreased by the capturing of the electron emitted from the source. The breakdown voltage is improved and the breakdown curve is obtained thanks to the acceptor-like trap. For the conventional structure without silicon doping in the AlGaN layer, the breakdown voltage is 296 V. The breakdown voltage is increased to 400 V for the $Al_{0.25}Ga_{0.75}N$/GaN HEMTs with partial silicon doping due to the new electric field peak. The uniform surface electric field is obtained by this new electric field peak to decrease the high electric field near the

gate electrode. The surface electric field distributions are shown in Fig. 5.

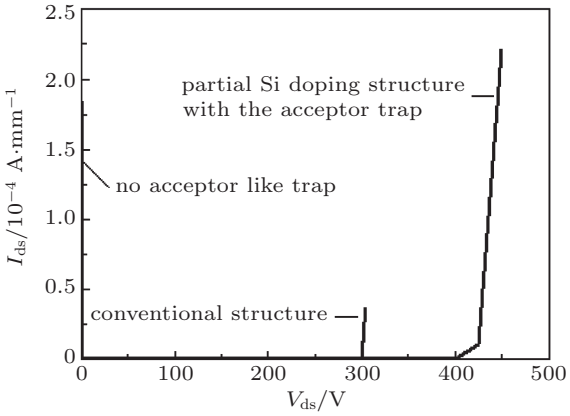


Fig. 4. The breakdown curve that is the same as the test results for the $Al_{0.25}Ga_{0.75}N$/GaN HEMTs with an acceptor-like trap.

Figure 5 shows the surface electric field distributions for the partial silicon doping and conventional $Al_{0.25}Ga_{0.75}N$/GaN HEMTs. When the $Al_{0.25}Ga_{0.75}N$/GaN HEMTs are in reverse bias, the voltage between the gate and drain electrodes is generated by the Schottky junction, and the voltage of the source and drain electrodes is assumed through the high resistivity GaN buffer layer after the 2DEG is depleted. These electric field distributions are similar to the silicon LDMOS. Two high electric field peaks are introduced near the gate and drain electrodes. The two electric field peaks are equal under the optimized conditions. Figure 5 shows the surface electric field of the conventional $Al_{0.25}Ga_{0.75}N$/GaN HEMTs. There are two distinct electric field peaks at the gate and drain edges.

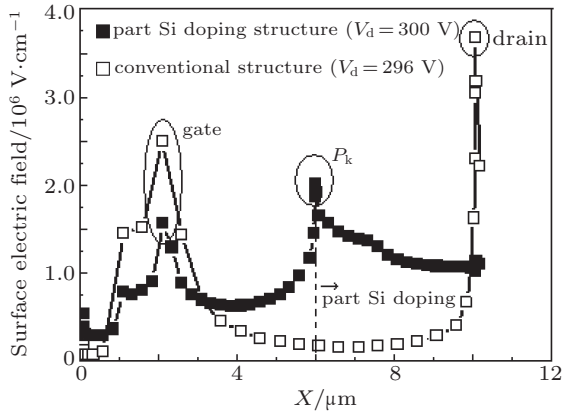


Fig. 5. The surface electric field of the conventional and partial silicon doping $Al_{0.25}Ga_{0.75}N$/GaN HEMTs.

The high electric field peak near the drain can be expressed by Fig. 6. The potential gradually increases from the source to the drain electrode along the channel after the 2DEG is depleted. It can be seen from Fig. 6 that the potential of point A is lower than that of B at the interface of AlGaN/GaN. However, the potential of point A' is equal to that of B' due to the drain electrode equipotential effect, which is the effect for the partial silicon doping AlGaN/GaN HEMTs shown in Fig. 1. Thus, the potential difference is formed between A' and A. This potential difference causes the equipotential line cluster and brings the high electric field peak near to the drain electrode. Drain field plate structures[2,21] have been proposed to optimize the high electric field near the drain. However, a physical explanation of the high electric field has not been obtained yet. In this paper, the reason for the high electric field peak has been explained for the first time, essentially by the potential difference distribution. The location of the high electric field is a breakdown point for power devices and results in a decline in reliability.

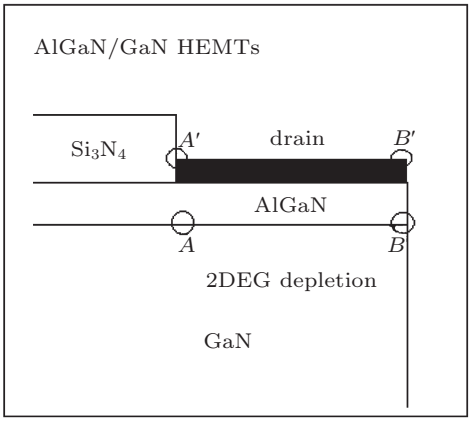


Fig. 6. Cross section of the drain electrode for the $Al_{0.25}Ga_{0.75}N$/GaN HEMTs.

For the partial silicon doping $Al_{0.25}Ga_{0.75}N$/GaN HEMTs, a new electric field peak is introduced in the middle of the low field region resulting from the positive charge in the AlGaN polarization layer. This new electric field peak decreases the high electric field near the gate and drain electrodes, and the electric field distribution tends to be optimized. When a positive charge is connected with the drain electrode, this new structure possesses not only the electric field modulation effect, but also the drain field plate effect.

When the drain voltage is 296 V, the high electric field peak for the conventional structure has reached the critical breakdown electric field of the GaN material (see Fig. 5). So, the device reaches the avalanche

break, and the breakdown voltage is 296 V for the conventional structure. The leakage current is small for the device's surface and substrate. However, for the partial silicon doping $Al_{0.25}Ga_{0.75}N$/GaN HEMTs, the electric field distribution is uniform. Its maximum electric field is only 2.0×10^6 V/cm as the drain voltage is 300 V, which has not yet reached the critical breakdown electric field of the GaN material. That is to say, the breakdown voltage will be greater than 300 V. This is the essence of the electric field modulation effect to improve the breakdown voltage.

Figure 7 shows the surface electric fields with different drain voltages for the partial silicon doping $Al_{0.25}Ga_{0.75}N$/GaN HEMTs. It can be seen from Fig. 7 that the electric field peak near the gate increases with the drain voltage. This high electric field is mainly attributed to the device avalanche in the conventional structure. The new electric field peaks of the partial silicon doping structure are almost equal for the different drain voltages of 300, 360, and 400 V. The surface electric field tends to be uniform due to the drain field plate effect. When the drain voltage is 400 V, the peak of the surface electric field has reached the critical breakdown electric field of the GaN material. The avalanche break occurs for the partial silicon doping $Al_{0.25}Ga_{0.75}N$/GaN HEMTs, and the breakdown voltage is 400 V. The breakdown voltage increases by about 35% compared with that of the conventional structure, which is 296 V.

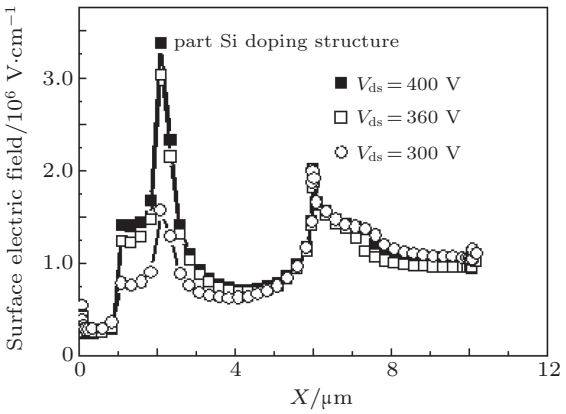


Fig. 7. Surface electric field distributions with different drain voltages of the partial silicon doping $Al_{0.25}Ga_{0.75}N$/GaN HEMTs.

Figure 8 shows the surface electric field distributions for the partial and complete silicon doping $Al_{0.25}Ga_{0.75}N$/GaN HEMTs. For the complete silicon doping structure, although the 2DEG concentration is larger than that of the partial silicon doping in the channel region, the surface field is a typical triangle. The highest electric field is at the gate edge near the drain electrode, and the electric field decreases sharply along the drift region. Avalanche breakdown occurs due to the reverse bias Schottky junction. The device reliability is affected by the hot electron effect resulting from the high electric field near the gate. The 2DEG concentration and output current decrease due to the triangle electric field distribution for the complete silicon doping $Al_{0.25}Ga_{0.75}N$/GaN HEMTs. The high electric field near the gate reaches about 4.8×10^6 V/cm for a 296 V drain voltage of the complete silicon doping structure, which exceeds the critical breakdown electric field of the GaN material. While for partial silicon doping, the new electric field peak is introduced in the surface electric field distribution due to the electric field modulation effect by the partial positive charge. The high electric field near the gate is decreased effectively. The critical breakdown electric field of the GaN material is reached when the drain voltage is 400 V for the partial silicon doping $Al_{0.25}Ga_{0.75}N$/GaN HEMTs. However, the electric field reaches 5.7×10^6 V/cm when the drain voltage is 400 V in the complete silicon doping $Al_{0.25}Ga_{0.75}N$/GaN HEMTs. This exceeds the critical breakdown electric field of the GaN material.

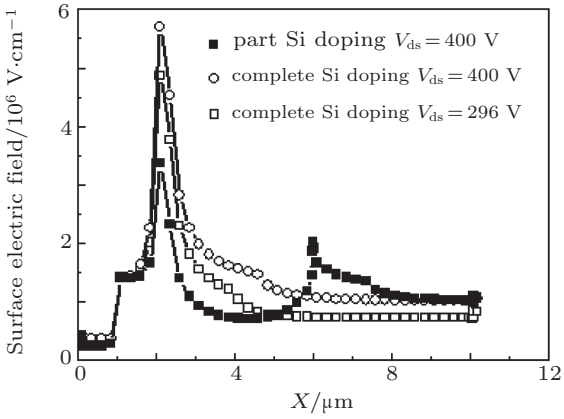


Fig. 8. Surface electric field distributions with different drain voltages of the $Al_{0.25}Ga_{0.75}N$/GaN HEMTs.

Figure 9 shows the I_{ds}–V_{ds} curves for the conventional and partial silicon doping $Al_{0.25}Ga_{0.75}N$/GaN HEMTs structures. It can be seen from Fig. 8 that the two kinds of devices are the depletion-mode $Al_{0.25}Ga_{0.75}N$/GaN HEMTs. The output current is related to the 2DEG concentration. For the partial silicon doping $Al_{0.25}Ga_{0.75}N$/GaN HEMTs, the output

current is larger than that of the conventional structure due to high 2DEG density.

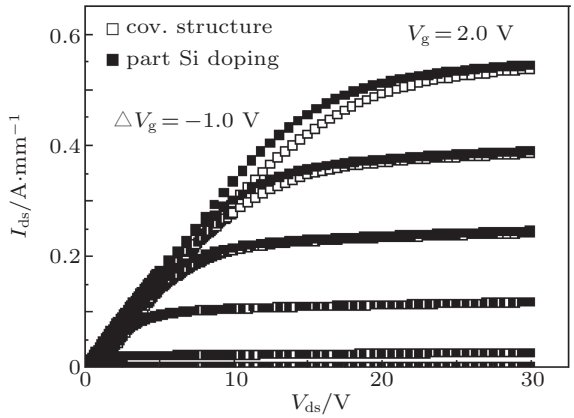


Fig. 9. I_{ds}–V_{ds} curves of the conventional and partial silicon doping $Al_{0.25}Ga_{0.75}N$/GaN HEMTs.

4. Experimental and measurement results

There are two commercial samples used in this paper for the experimental and measurement results. One is the conventional wafer with un-doped $Al_{0.25}Ga_{0.75}N$/GaN, and the other is the complete silicon doping in the $Al_{0.25}Ga_{0.75}N$/GaN HEMTs. For the two samples, the epitaxial structure contains a GaN buffer and a 20 nm AlGaN layer. Firstly, mesa isolations were carried out by inductively coupled plasma reactive ion etching. Secondly, the ohmic contacts were formed simultaneously by the e-beam deposition of Ti/Al/Ni/Au (20 nm/120 nm/50 nm/80 nm) and subsequent rapid thermal annealing (RTA) at 850 °C for 30 s. Thirdly, the Schottky contacts were defined by the photolithography and subsequent CF_4 plasma treatment at 120 W for 180 s. Then, the samples were annealed at 400 °C for 10 min to repair the plasma-induced damage in the AlGaN layers. The negatively charged fluorine ions effectively depleted the 2DEG, and the threshold voltages are shifted to 0.68 V and 0.509 V for the conventional structure with un-doped and complete silicon doping at the AlGaN layer samples, respectively. Finally, the self-aligned Schottky contacts were deposited by e-beam evaporation of Ni/Au and liftoff.

The transfer characteristics of I_{ds} and V_g are shown in Fig. 10. It shows that the threshold voltage is 0.68 V for the conventional structure (Fig. 10(a)), and 0.509 V for the complete silicon doping $Al_{0.25}Ga_{0.75}N$/GaN HEMTs (Fig. 10(b)). The two devices are both of depletion-mode operation, which is obtained by CF_4 plasma treatment at 120 W for 180 s. The fluorine ions with the negative charge deplete the 2DEG.[3] The 2DEG density is lower in the conventional structure than in the complete doping one, and therefore the 2DEG is depleted effectively for the former, which causes a higher threshold voltage compared with the latter.

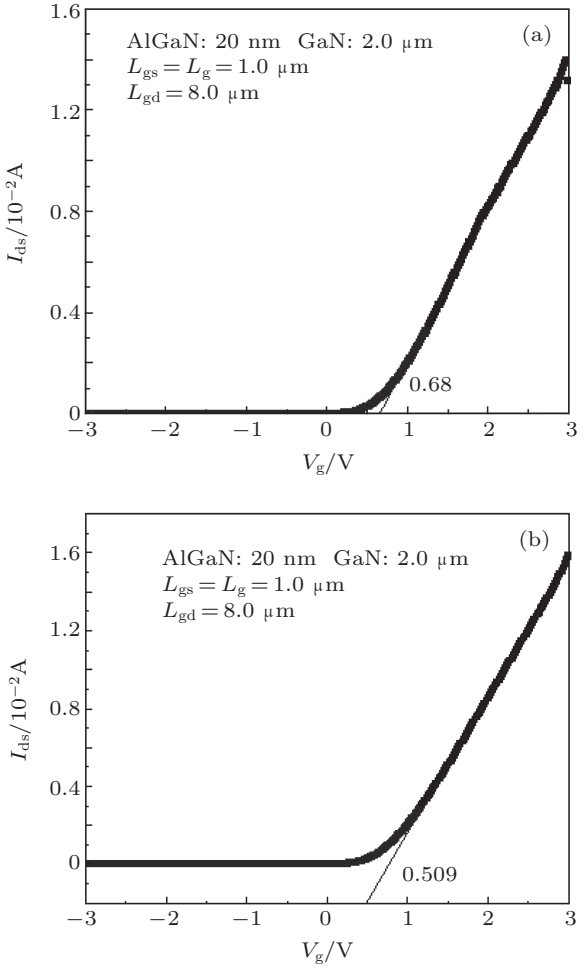


Fig. 10. The transfer characteristics for (a) the conventional structure with an V_{th} of 0.68 V and (b) the complete silicon doping structure with V_{th} of 0.509 V.

Figure 11 shows the measured forward dc-output characteristics for both the conventional and complete silicon doping $Al_{0.25}Ga_{0.75}N$/GaN HEMTs structures. The I_{ds} is lower for the former than that of the latter due to the high 2DEG density. This reveals that the two devices are depletion-mode AlGaN/GaN HEMTs because of the positive threshold voltages (Fig. 10). The output current of the complete silicon doping structure is 338 mA/mm for V_g = 2 V, which is greater than that of its conventional counter-

part (294 mA/mm).

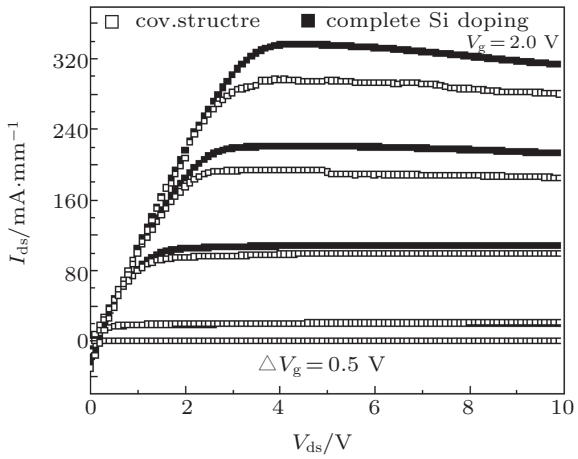


Fig. 11. The I_{ds}–V_{ds} output characteristics of conventional and complete silicon doping $Al_{0.25}Ga_{0.75}N$/GaN HEMTs.

Figure 12 shows the reverse blocking characteristics for the conventional and complete silicon doping AlGaN/GaN HEMTs. BV is defined as the voltage, with the drain leakage current reaching 1 mA/mm. The value of BV is 308 V in the conventional structure with an un-doped AlGaN layer of $Al_{0.25}Ga_{0.75}N$/GaN HEMTs, which is higher than that of 210 V in the complete silicon doping at the $Al_{0.25}Ga_{0.75}N$ layer. It is more difficult to deplete 2DEG bearing reverse bias in the complete silicon doping structure than in the conventional structure due to the high 2DEG density. However, a large forward current can be obtained for the high 2DEG in the complete silicon doping structure, which is shown in Fig. 11.

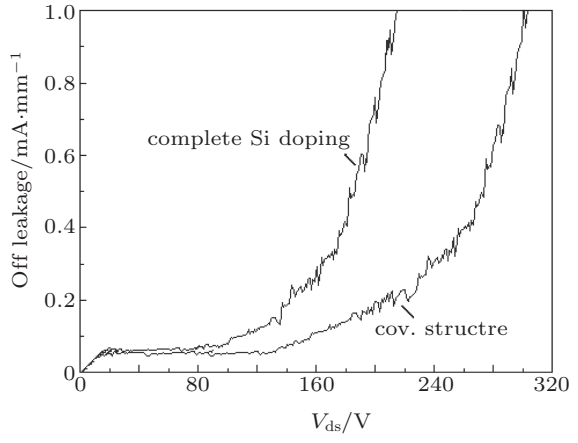


Fig. 12. Measured output characteristics for the conventional and complete silicon doping structures at reverse bias.

5. Conclusions

In this paper, a novel $Al_{0.25}Ga_{0.75}N$/GaN HEMT has been proposed with partial silicon doping in the $Al_{0.25}Ga_{0.75}N$ layer applying the electric field modulation effect. For the first time, the electric field peak near the drain is explained by the potential difference between the drain electrode and GaN surface. Simulated breakdown curves the same as the examination results are obtained for the first time by introducing an acceptor-like trap into the N-type GaN buffer. The surface electric field of the proposed structure is optimized to be uniform due to the new electric field peak by the positive charge of the part silicon. The breakdown voltage is improved because of the decreased high electric field near the gate edge, and increases from 296 V to 400 V for the partial silicon doping $Al_{0.25}Ga_{0.75}N$/GaN HEMTs compared with the conventional structure. The resistance of the channel region is decreased in the partial silicon doping $Al_{0.25}Ga_{0.75}N$/GaN HEMTs due to high 2DEG concentration, which increases the output current. The reliability caused by the hot electron is improved due to uniform surface electric field distribution.

References

[1] Zhang A P, Johnson J W and Ren F 2001 *Appl. Phys. Lett.* **78** 823
[2] Saito W, Kuraguchi M, Takada Y, Tsuda K, Omura I and Ogura T 2005 *IEEE Trans. Electron Devices* **52** 106
[3] Song D, Liu J, Cheng Z Q, Tang W C W, Lau K M and Chen K J 2007 *IEEE Electron Device Lett.* **28** 189
[4] Ando Y, Okamoto Y, Miyamoto H, Nakayama T, Inoue T and Kuzuhara M 2003 *IEEE Electron Device Lett.* **24** 289
[5] Wu Y F, Saxler A, Moore M, Smith R P, Sheppard S, Chavarkar P M, Wisleder T, Mishra U K and Parikh P 2004 *IEEE Electron Device Lett.* **25** 117
[6] Tipirneni N, Koudymov A, Adivarahan V, Yang J, Simin G and Asif Khan M 2006 *IEEE Electron Device Lett.* **27** 716
[7] Arulkumaran S, Egawa T, Ishikawa H and Jimbo T 2003 *Appl. Phys. Lett.* **82** 3110
[8] Bardwell J A, Haffouz S, McKinnon W R, Storey C, Tang H, Sproule G I, Roth D and Wang R 2007 *Electrochem. Solid-State Lett.* **10** H46
[9] Chattopadhyay M K and Tokekar S 2008 *Microelectron. J.* **39** 1181
[10] Arulkumaran S, Liu Z H, Ng G I, Cheong W C, Zeng R, Bu J, Wang H, Radhakrishnan K and Tan C L 2007 *Thin Solid Films* **515** 4517
[11] Jha S, Jelenkovic E V, Pejovic M M, Ristic G S, Pejovic M, Tong K Y, Surya C, Bello I and Zhang W J 2009 *Microelectron. Eng.* **86** 37

[12] Chen X B and Johnny K O S 2001 *IEEE Trans. Electron Devices* **48** 344

[13] Sameh G, Nassif K and Salama C A T 2003 *IEEE Trans. Electron Devices* **50** 1385

[14] Duan B X, Zhang B and Li Z J 2005 *Solid-State Electron.* **49** 1965

[15] Duan B X, Zhang B and Li Z J 2006 *IEEE Electron Device Lett.* **27** 377

[16] Duan B X, Yang Y T, Zhang B and Hong X F 2009 *IEEE Electron Device Lett.* **12** 1329

[17] Duan B X, Yang Y T and Zhang B 2009 *IEEE Electron Device Lett.* **30** 305

[18] Duan B X, Yang Y T and Zhang B 2010 *Solid-State Electron.* **54** 685

[19] Saito W, Takada Y, Kuraguchi M, Tsuda K, Omura I, Ogura T and Ohashi H 2003 *IEEE Trans. Electron Devices* **50** 2528

[20] Koudymov A, Adivarahan V, Yang J, Simin G and Asif Khan M 2005 *IEEE Electron Device Lett.* **26** 704

[21] Karmalkar S, Deng J Y, Shur M S and Gaska R 2001 *IEEE Electron Device Lett.* **22** 373

[22] ISE TCAD Manuals, release 10.0.

[23] Zhang S, Sin J K O, Lai T M L and Ko P K 1999 *IEEE Trans. Electron Device* **46** 1036

[24] Hardikar S, Tadikonda R, Green D W, Vershinin K V and Sankara Narayanan E M 2004 *IEEE Trans. Electron Device* **51** 2223

[25] Heikman S, Keller S, DenBaars S P and Mishra U K 2002 *Appl. Phys. Lett.* **81** 439

[26] Tang H, Webb J B, Bardwell J A, Raymond S, Salzman J and Uzan-Saguy C 2001 *Appl. Phys. Lett.* **78** 757

[27] Webb J B, Tang H, Rolfe S and Bardwell J A 1999 *Appl. Phys. Lett.* **75** 953

[28] Katzer D S, Storm D F, Binari S C, Roussos J A, Shanabrook B V and Glaser E R 2003v *J. Cryst. Growth* **251** 481

[29] Poblenz C, Waltereit P, Rajan S, Heikman S, Mishra U K and Speck J S 2004 *J. Vac. Sci. Technol.* B **22** 114